Published in final edited form as:
Biomed Microdevices. 2011 December ; 13(6): 1033–1042. doi:10.1007/s10544-011-9573-z.

Purification of cell subpopulations via immiscible filtration assisted by surface tension (IFAST)

Scott M. Berry,
Department of Biomedical Engineering, University of Wisconsin-Madison, 1111 Highland Ave., Madison, WI 53705, USA; Carbone Cancer Center and Wisconsin Institutes for Medical Research, University of Wisconsin-Madison, 1111 Highland Ave., Madison, WI 53705, USA

Lindsay N. Strotman,
Department of Biomedical Engineering, University of Wisconsin-Madison, 1111 Highland Ave., Madison, WI 53705, USA; Carbone Cancer Center and Wisconsin Institutes for Medical Research, University of Wisconsin-Madison, 1111 Highland Ave., Madison, WI 53705, USA

Jessica D. Kueck,
Carbone Cancer Center and Wisconsin Institutes for Medical Research, University of Wisconsin-Madison, 1111 Highland Ave., Madison, WI 53705, USA; Department of Oncology, University of Wisconsin-Madison, 1111 Highland Ave., Madison, WI 53705, USA

Elaine T. Alarid, and
Carbone Cancer Center and Wisconsin Institutes for Medical Research, University of Wisconsin-Madison, 1111 Highland Ave., Madison, WI 53705, USA; Department of Oncology, University of Wisconsin-Madison, 1111 Highland Ave., Madison, WI 53705, USA

David J. Beebe
Department of Biomedical Engineering, University of Wisconsin-Madison, 1111 Highland Ave., Madison, WI 53705, USA; Carbone Cancer Center and Wisconsin Institutes for Medical Research, University of Wisconsin-Madison, 1111 Highland Ave., Madison, WI 53705, USA

Abstract

The selective isolation of a sub-population of cells from a larger, mixed population is a critical preparatory process to many biomedical assays. Here, we present a new cell isolation platform with a unique set of advantages over existing devices. Our technology, termed Immiscible Filtration Assisted by Surface Tension, exploits physical phenomena associated with the microscale to establish fluidic barriers composed of immiscible liquids. By attaching magnetically-responsive particles to a target cell population via immunocapture, we can selectively transport this population across the immiscible barrier and into a separate aqueous solution. The high interfacial energy associated with the immiscible phase / aqueous phase boundaries prevents unwanted cells or other contaminants from inadvertently crossing the immiscible phase. We have demonstrated, using fluorescent particles, stromal cells, and whole blood as “background”, that we can successfully isolate ~70% of a target breast cancer cell population with an average purity of >80%. Increased purity was obtained by coupling two immiscible barriers in series, a modification that only slightly increases operational complexity. Furthermore, several samples can be processed in parallel batches in a near-instantaneous manner without the requirement of any washing, which can cause dilution (negative selection) or

djbeebe@wisc.edu .

Electronic supplementary material The online version of this article (doi:10.1007/s10544-011-9573-z) contains supplementary material, which is available to authorized users.

significant uncontrolled loss (positive selection) of target cells. Finally, cells were observed to remain viable and proliferative following traverse through the immiscible phase, indicating that this process is suitable for a variety of downstream assays, including those requiring intact living cells.

Keywords

Cell sorting; Microfluidics; Immiscible phase filtration; IFAST

1 Introduction

The ability to isolate a specific sub-population of cells from a mixed population is a fundamental process utilized in both clinical and biomedical research settings. Demands for higher separation efficiency, improved process flexibility, reduced cost and complexity, and increased throughput have led to a proliferation of innovative separation techniques. Traditional methods, including centrifugation (e.g. Ficoll-based stratification) and membrane filtration (Tsutsui and Ho 2009), have been supplemented by newer techniques that have higher sensitivity and throughput, including fluorescence–activated cell sorting (FACS) and magnetic cell sorting. More recently, miniaturized versions of these techniques have emerged which are enhanced by the intrinsic advantages of microfluidics, including lower manufacturing and operational costs, reduced sample and reagent volumes, increased automation potential, accelerated time-to-results, and portability. In addition, microfluidic systems have been developed that utilize active (e.g. dielectrophoresis (Hu et al. 2005), electrophoresis (Fu et al. 1999), optical trapping (MacDonald et al. 2003), or acoustic force (Petersson et al. 2007)) or passive processes (e.g. micro-sieving (Tsutsui and Ho 2009), channel geometry (Huang et al. 2004; Wildings et al. 1998), hydrodynamic forces (Yamada et al. 2004), immunocapture (Nagrath et al. 2007)) to selectively isolate a sub-population of cells. Reviews of cell sorting processes have been recently published by Tsutsui and Ho (2009), Bhagat et al. (2010), and Lenshof and Laurell (2010).

Magnetic cell separation has become popular among researchers for a variety of reasons including high sorting efficiency, parallel processing, and relative insensitivity to fluctuations in processing conditions (Pamme 2005). First introduced by Miltenyi et al. (1990), magnetic cell separation operates by binding paramagnetic particles (PMPs) to cells-of-interest using a PMP-immobilized antibody that recognizes a cell-specific surface antigen. A magnetic field selectively actuates the PMP-labeled sub-population and isolates them from the remainder of the sample. The mechanism by which this isolation occurs can be further categorized into either batch processing or continuous flow. In batch processing, popular with commercial systems (Including CELLection (Invitrogen), MACS (Miltenyi), IMAG (BD Biosciences), EasySep (Stem Cell Technology), and MagCellect-beads (R&D systems)), a magnet is applied to temporarily immobilize the magnetically-responsive cells, enabling the washing away of the remainder of the sample (a process known as “magnetic pull-down”). While advantageous for rapid separation, it has shown low sensitivity, especially for capturing rare cell populations (Miltenyi et al. 1990) that can become lost during washing. Continuous flow cell sorting, popular with emergent microfluidic technologies, utilizes a magnetic field to cause PMP-labeled cells within a moving stream to alter their direction of flow, thus channeling them away from the bulk of the sample (Xia et al. 2006; Pamme and Manz 2004). However, continuous flow processes can be expensive and operationally complex as a liquid handling infrastructure (i.e. pumps, flow controllers, tubing, etc.) is required to drive flow.

In this manuscript, we adapt a previously developed magnetic separation protocol, termed IFAST (Immiscible Filtration Assisted by Surface Tension), in order to separate a target cell population from a bulk solution. The foundation of this technology is immiscible phase filtration, a rapid purification technique developed by our group and others to isolate nucleic acids (Sur et al. 2010; Berry et al. 2011; Bordelon et al. 2011), proteins (Shikida et al. 2006; Chen et al. 2010), and cells/lysates (Kelso et al. 2009). This methodology uses a magnet to draw PMP-bound analyte through an immiscible barrier (e.g. oil, wax, organic solvent) that separates an aqueous sample from an aqueous output buffer (Fig. 1(a)–(c)). In macroscale versions of this technology, aqueous and oil phases stratify based on density, with a less dense oil phase floating above two adjacent wells containing aqueous reagents (Sur et al. 2010; Kelso et al. 2009). However, when the interfacial area is reduced to microscale, the relative influence of surface tension on the fluid mechanics of a system is increased (Berry et al. 2011; Chen et al. 2010), thus enabling the “pinning” of liquids within certain regions using surface tension (Zhao et al. 2001; Atencia and Beebe 2005; Cho et al. 2007). This phenomenon, which is characterized by the dimensionless Bond number, facilitates side-by-side loading of reagents and simplification of the device geometry (from 3D to planar), thereby enabling operation with a single move of a magnet. In past works (Sur et al. 2010; Berry et al. 2011; Chen et al. 2010), immiscible phase filtration has led to high quality purification of nucleic acid and protein analytes using a process that is significantly faster and simpler than washing-based protocols. Here, we evaluate the application of this technique to cell sorting and compare results to a traditional washing process.

2 Experimental

IFAST device fabrication

The IFAST platform was designed to mimic the footprint of a standard 384-well microtiter plate in order to facilitate compatibility with existing laboratory infrastructure (e.g. multichannel pipettes, liquid handling robots, plate readers) and to increase familiarity for potential users in the biomedical sciences (Fig. 1(d)). The devices were fabricated from polydimethyl siloxane (PDMS; Sylgard 184, Dow Corning) using soft lithographic techniques. Briefly, layers of a UV-curable epoxy (SU-8 100, Microchem) were spun onto a silicon wafer and patterned by using a mask to selectively expose the epoxy to UV light. Uncured epoxy was removed by washing with ethylene glycol followed by rinsing with isopropyl alcohol to complete formation of the epoxy mold. Uncured PDMS was poured on the mold and cured for 4 h at 85°C. Cured PDMS was peeled off the mold and bonded to glass (Cover Glass, Thermo Scientific) using an oxygen plasma to enhance bonding. Each assay consists of three (single oil barrier) or five (double oil barrier) wells oriented in a line, where the well-to-spacing is 4.5 mm. Since a planar process of soft lithography was employed, the total well height was only 750 μm, which is significantly shorter than a microtiter plate, resulting in a well volume of ~10 μL. Unlike microtiter plates, the wells are connected in sequence by a series of microfluidic constrictions (constriction measures 0.5 μm by 0.25 μm). These constrictions are small enough to act as pinning locations, preventing reagents from exiting their wells during filling, while allowing PMPs (and material captured on the PMP surface) the ability to move from well to well in response to a magnetic field. Because the device was engineered to mimic the footprint of a 384-well plate, it is compatible with existing well plate-based infrastructure such as multi-channel pipettes and liquid handling robots.

Preparation of PMPs

60 μL of a stock solution (10 mg/mL) of 2.8 μm-diameter, Streptavadin-coated paramagnetic particles (PMPs; Dynabeads M-280 Streptavadin, Invitrogen) were transferred to a 1.5 mL microcentrifuge tube. A magnet (BX041, K&J Magnetics) was used to

aggregate the PMPs against the side of the tube and the supernatant was removed with a pipette. The PMPs were washed once with PBS, re-suspended in 80 μL of fresh PBS and mixed with 7.5 μL of a 0.2 mg/mL solution of biotinylated EpCAM antibody (ab79079, Abcam). The PMP / antibody mixture was incubated for 30 min at room temperature with rocking. After incubation, the PMPs were washed four times with 80 μL of 0.1% bovine serum albumin (BSA) in PBS then re-suspended in 80 μL of 0.1% BSA in PBS with 2 mM ethylenediaminetetraacetic acid (EDTA).

Cell culture

Human breast cancer epithelial cells (MCF-7) engineered to stably express green fluorescent protein (GFP) and human bone marrow stromal cells (HS-5) were cultured in Dulbecco's modified Eagle's medium (DMEM; Mediatech) supplemented with 10% fetal bovine serum (FBS; HyClone). Cell media was changed every 2–4 days and cells were passaged every 4–7 days. For experimentation, cells were incubated in 0.05% trypsin / EDTA for 15–20 min then agitated with a pipette to ensure complete release and dispersion of cells in solution. Cells were counted with a hemocytometer, centrifuged for 3 min, and re-suspended in media at a concentration of 2 million cells per mL.

Cell capture

For each experiment 20 μL of antibody-labeled PMPs (prepared as previously described) were mixed with 20 μL of MCF-7 cell suspension (either used at 2 million / mL or further diluted in media) in a 1.5 mL microcentrifuge tube that had been pre-coated with a solution of 1% BSA (to block against adhesion with the tube sidewalls). For characterization experiments, 20 μL of a solution of fluorescent particles (1 million beads / mL washed twice in PBS; 15 μm diameter Fluospheres, Molecular Probes F8843) was added to the mixture as well. In other experiments, 20 μL of a HS-5 cell suspension (concentration of 2 million cells / mL) or 20 μL human blood (obtained according to IRB-approved protocol) was added to the PMP / cell suspension mixture. In all cases, the mixtures were incubated for 30 min at 4°C with gentle rocking to promote immunocapture of the target cells by the PMPs. More vigorous mixing resulted in substantial lysis of the cells.

Device filling and operation

For each separation, 8.5 μL of one of the cell / PMP mixtures prepared in the previous section was added to the input port of an IFAST device. 8.5 μL of PBS was added to the output port and 8.5 μL of oil (Olive oil, Unilever) was added to the center port of the IFAST device to complete device filling. In cases where two oil traverses were performed in series, the middle well was loaded with a wash buffer (PBS with 0.01% Tween 20) after the input and output wells were loaded as previously described. In all cases, the oil well(s) were filled last since the low surface tension of the oil is insufficient to pin flow at the microfluidic constrictions. To operate the device, it was placed on a magnetic bar (NdFeB N52 Magnet, K&J Magnetics) such that the PMPs in the input well aggregated above the bar. The device was then moved at an approximate rate of 1 cm/s such that the PMPs (and attached cells) were drawn through the oil phase and into the PBS (Fig. 1, Supplementary Video 1). Supplementary Video 1 illustrates that the entire loading and operation of an array of five IFAST devices can be performed in less than 80 s. In cases where two traverses were performed, the device was removed from the magnet and the PMP/cell aggregate was briefly dispersed in the wash buffer (t=5 s) with a micropipette before reapplying the magnetic field and performing the second traverse. Once in the output well, the PMP/ cell aggregate was dispersed with a micropipette, thus homogenously distributing the well contents in order to facilitate imaging and accurate quantification. Typically, arrays of 5 to 8 adjacent devices were operated simultaneously using a longer magnetic bar (as in Supplemental Video 1). To characterize performance of the IFAST platform, MCF-7 cells at a concentration of 2

million cells / mL were mixed with fluorescent particles at a concentration of 1 million particles / mL. To demonstrate the ability of the IFAST to isolate smaller subpopulations of cells (as with “rare” cell types), the concentration of MCF-7 cells was reduced to 100,000 cells / mL. A minimum of three separations were performed with each concentration using both the single and double oil barrier IFAST platforms. In addition, 8.5 μL of each solution was loaded into multiple IFAST wells to confirm the ratios were accurate (i.e., no significant cell lysis during experimental setup). All experiments were performed within 3 h of removing the cells from the incubator as significant lysis was observed after this time period as indicated by the release of GFP from lysed cells into the surrounding liquid. As a control, PMP-bound cells were washed three times with PBS. Each wash involved magnetically aggregating the PMP-bound cells against the side of a 1.5 mL microcentrifuge tube, aspirating the supernatant, then re-suspending the aggregate in fresh buffer. In preliminary washing trials, it was observed that the recovery of cells was dependent on the vigorousness of the re-suspension step. Therefore, multiple re-suspension methodologies were tested. To simulate “vigorous” washing, the wash buffer was pipetted directly onto the aggregate, instantly breaking it up. To simulate “gentle” washing, the wash buffer was slowly pipette against the wall of the microcentrifuge tube above the aggregate, such that the wash buffer trickled down the tube wall and slowly dispersed the aggregate.

Measurement and analysis

Following the characterization experiments, each well of each device was measured with a fluorescent microscope (Olympus IX71) using excitation wavelengths of 492 nm (MCF-7 cells) and 572 nm (fluorescent particles). For the experiments involving stromal cells or blood, each well was imaged with phase contrast as well as fluorescence using excitation at 492 nm. After traverse, devices were given ~15 min before imaging to allow cells and particles to settle to the bottom of each well such that all cells and particles were in a single focal plane. Imaging was done with a 4× objective which resulted in a field of view in each image that was approximately 30% of the total well area. Images were processed with ImageJ software (Abramoff et al. 2004) to determine counts for both cells and particles. Briefly, rolling ball filter and de-speckling algorithms (both included with ImageJ) were employed to remove background noise from each image. Because the fluorescent particles were visible in the cell (492 nm) images due to some fluorescence in this spectrum, the particle (572 nm) images were subtracted from the cell images to prevent particles from being double counted as both cells and particles. Last, the Find Maxima algorithm (also included with ImageJ) was used to count the number of cells or particles in each image. Representative images (both fluorescence and fluorescence overlaying phase contrast) were counted manually to ensure the software-based counting was within 5% of the actual values. Cell recovery was determined by calculating the fraction of MCF-7 cells in the output well relative to the total number of MCF-7 cells in an image of the unsorted solution. Purity was calculated as:

$$\text{Purity} = \frac{N_{\text{OutputCells}}}{N_{\text{OutputCells}} + N_{\text{OutputParticles}}} \quad (1)$$

where $N_{\text{OutputCells}}$ is the number of target cells in an image of the output well and $N_{\text{OutputParticles}}$ is the number of fluorescent particles in the same output well image.

Cell viability

Following traverse of the oil barrier, cells from some devices were removed from the output wells and seeded into 100 μL of media (DMEM) in a 96-well plate. Typically, output wells from two devices were pooled before loading into the well plate to increase cell density. Similar numbers of cells that were not bound to PMPs or were bound to PMPs, but not

traversed through oil, were seeded into other wells of the 96-well plate for comparison. These cells were imaged with bright field and fluorescent (492 nm) microscopy 4 to 24 h after seeding to confirm cellular attachment to the well plate surface. Following cellular attachment, the cells were washed twice with media to remove unbound PMPs or residual fluorescent particles from the system. Some wells were stained with 4 μM ethidium homodimer-1 (from LIVE/DEAD Viability / Cytotoxicity Kit for mammalian cells, Invitrogen) to selectively label dead cells (those with permeable membranes). These wells were fluorescently imaged at 572 nm to identify dead cells and the dead cell count was normalized by the integrated intensity of the green fluorescent signal, which was found to be directly proportional to cell number (Fig. S-1). Other wells were allowed to incubate for 3–4 days to confirm cell proliferation following passage through the oil barrier. These wells were imaged a second time with bright field and fluorescent microscopy (492 nm) and compared against the images recorded initially after seeding.

3 Results and discussion

MCF-7 cells were successfully attached to PMPs via an EpCAM antibody and pulled across the oil barrier to separate them from fluorescent spheres (Fig. 2). The total time required to load and operate a single device was typically less than 30 s and an array of five devices was loaded and operated in approximately 80 s. Both cell and particle loss was quantified. While, the majority of the cells traversed the oil barrier into the output well, a minority (16% average over 18 trials) typically remained in the input well. Inspection of these cells showed few or no visible bound PMPs and further manipulation with a magnet demonstrated that they were unresponsive to a magnetic field, suggesting that the unsorted cells failed to bind with PMPs. When using two oil barriers in series, the majority of MCF-7 cells were successfully transferred to the output well, but a small fraction of cells (7% average over 9 trials) remained in the middle well (wash buffer). These cells were found to be unresponsive when exposed to a magnetic field,suggesting that either the bound PMPs had been sheared off the cells during mixing or the cells never bound to PMPs, but were initially trapped in the volume of the PMP aggregate and drawn across the first oil barrier, only to be liberated from the aggregate during mixing. When no immiscible phase liquid is added to the device (leaving an air gap between the input and output wells), the PMP / cell aggregate becomes stuck against the device surface as soon as the aggregate exits the aqueous phase of the input well as the immiscible phase also acts as a lubricant to facilitate transfer of the aggregate from the input to the output of the device. There was a surplus of unbound PMPs in all cases, suggesting that sufficient binding capacity was available to capture all cells. Other possible factors that may limit attachment of PMPs to MCF-7 cells include cleaving of EpCAM during trypsinization, low EpCAM expression on a subpopulation of cells, or low antibody affinity.

Recovery of the MCF-7 cells was found to be higher when using the IFAST devices compared to traditional washing (Fig. 3(a)). Furthermore, recovery was found to be dependent on the vigorousness of the washing steps. Specifically, recovery was reduced 4-fold when using “vigorous” washing as opposed to “gentle” washing (as defined in the Section 2). The error introduced by this difficult-to-control variable illustrates an advantage of the IFASTsystem, which exhibited very low variance between trials due to the elimination of the strongly user-dependent washing steps. When using a lower ratio of MCF-7 cells to fluorescent particles (1:10 as opposed to 2:1, as shown in Fig. 2(d)), the IFASTcontinued to recover the majority of the cells (an average of only 7% of the MCF-7 cells remained in the input well after IFAST operation), suggesting that the IFAST is also appropriate for isolating minority sub-populations of cells from samples.

The purity of the sorted cells was measured by counting the number of fluorescent particles that were inadvertently transferred to the output well. Adding a second oil barrier to the system significantly improves purity ($p<0.005$; Fig. 3 (b)) as most of the fluorescent particles that pass through the first oil barrier remain in the middle well and do not cross the second barrier (Fig. 2(c, d)). Comparison of the output well image of the single oil barrier (Fig. 2(a)) and the middle well images of the double oil barrier (Fig. 2(c, d)) shows a similar number of fluorescent particles. Since each of these images corresponds to one oil barrier traverse, this observation suggests that the fold purification obtained by crossing one oil barrier remains fairly constant (an average of a 98-fold reduction in fluorescent particles per traverse). Following one oil traverse, there were less than 30 fluorescent particles remaining in all trials. Typically, there were 1 or 2 (average of 1.7) particles transferred through both oil barriers and into the output well. Specifically, in trials involving the 1:10 ratio of cells to fluorescent particles, the purity was increased from 76% for one oil barrier to 99% when using two oil barriers. While the level of purity obtained by two oil traverses may not be required for all applications, it may have higher impact when the number of target cells is low, such that only a few contaminant particles will substantially decrease purity (since purity is a function of target cell number, Eq. 1).

We hypothesize that the major mechanism by which the fluorescent particles (or other contaminants) traverse an oil barrier is that they become trapped in the interstitial space of the PMP / cell aggregate. Using the concentrations and volumes of the PMPs and MCF-7 cells (assumed to be spheres with 20 μm diameters, as measured via microscopy using the 15 μm diameter of the fluorescent particles as a standard length), we can estimate the volume of the aggregate. Assuming a close-packing configuration, in which 26% of the aggregate volume is interstitial space and 74% is the volume of the aggregate components, we can estimate the minimum interstitial space volume (on the order of tens of nanoliters in our trials). Comparison of this volume to the total well volume (8.5 μL) elucidates the minimum fraction of material from the input well that becomes trapped in the interstitial space of the aggregate and traverses an oil barrier (e.g. If the interstitial space volume is 85 nL, then 1% of the total 8.5 μL input well volume will become trapped in the aggregate, resulting in 100-fold enrichment in purity). Mathematically, this concept is represented as:

$$\text{Theoretical Fold Contaminant Removal} = \frac{V_{\text{Device Packing}}}{N_{\text{Cells}} V_{\text{SinglrCell}} + V_{PMPs}} \quad (2)$$

where V_{Device} is the volume of the well (8.5 μL), $\phi_{Packing}$ is the packing ratio (0.74 for the ideal case of close-packed spheres), N_{Cells} is the number of cells in the well, $V_{SingleCell}$ is the volume of a single cell, and V_{PMPs} is the volume of the PMPs in each well (held constant at 14 nL). Equation 2 is plotted as a function of N_{Cells} on Fig. 3(c) along with the actual fold reduction in fluorescent particles for each trial of the characterization study. Note that the experimental data approaches, but does not exceed, the theoretical predictions. Some of the discrepancy between experiment and theory is likely due to non-ideal packing, in which the interstitial space of the aggregate is above 26% and $\phi_{Packing}$ is reduced. While the aggregate in the oil appears to be relatively tightly packed (as in Fig. 2(b)), the aggregate spreads along the floor of the device when in the aqueous phase. The collapse of the spread aggregate into the tightly-packed aggregate likely draws larger contaminants (such as the fluorescent particles) into the aggregate as it crosses the interface into the oil and becomes spheroid. Additional discussion of the general mechanics of the IFAST platform, specifically regarding the physics of device filling and operation, can be found in our previous publication (Berry et al. 2011).

The characterization experiments summarized in Figs. 2 and 3 demonstrate that the IFAST platform can effectively isolate a population of cells from background contaminants. In

these experiments, fluorescent microspheres were chosen as the background contaminant due to their relative inertness with the MCF-7 cells. In applications involving selection of a sub-population of cells (based expression of specific surface proteins) from a background composed of one or more other cell types, non-specific interactions will also influence the performance of the device. However, given that non-specific interaction will affect all immunocapture-type separation protocols, we wished to decouple these effects from the effects specific to the IFAST platform, thus presenting a more generalized characterization that is independent of biases associated with specific cells, expression of surface protein, or antibodies.

Following characterization, the sorting of a specific subpopulation of cells from a mixture of multiple cell types was demonstrated by using the IFAST platform to separate fluorescent breast cancer epithelial cells (MCF-7) from stromal cells (HS-5). A similar mixture may be encountered when attempting to analyze or process a biopsied tumor as cancer and stromal cells make up a substantial proportion (often the majority) of the cells present in the biopsied sample (Symmans et al. 2003). In our experiment, cell mixtures containing an average of 43% MCF-7 cells and 57% stromal cells were mixed with anti-EpCAM coated PMPs and loaded into single-barrier IFAST devices, which were operated as previously described. Following traverse of the immiscible phase barrier, an average of 85% of the MCF-7 cells were successfully recovered in the output well while only 11% of the HS-5 cells crossed the barrier, resulting in an average purity of 80% (Fig. 4(a-d)). These values were not substantially different than those reported in the characterization trials with fluorescent particles, suggesting that the presence of actual cells does not compromise IFAST performance, although this observation is likely dependent on the specific antibody used and specific interactions between the cell types that are used. Additionally, following traverse of the oil barrier, the input well of the IFAST device contained a population of HS-5 cells that had an average purity of 96% over 5 trials (Fig. 4 (b)), demonstrating how this device can simultaneously used for both positive and negative selection (i.e., the HS-5 population was not discarded during a wash).

To demonstrate the ability of the IFAST platform to sort a specific sub-population of cells from a complex environment, MCF-7 cells were spiked into whole human blood and mixed with anti-EpCAM coated PMPs (Fig. 4(e-h)). Using the single oil barrier IFAST, an average of 70% of the MCF-7 cells were recovered. However, due to the extremely high number of cells in whole blood, the output well of the IFAST contained a substantial number of non-MCF-7 cells (Fig. 4(e)). In these cases, purity was typically less than 10% as measured by manual counting of the non-fluorescent cells. This low performance was remedied by employing the IFAST configuration with two oil barriers as the vast majority of contaminant cells were released in the middle well of the device (Fig. 4(f)), resulting in a relatively pure population of MCF-7 cells in the output well (Fig. 4(g)). Purity was difficult to quantify as no non-fluorescent cells could be located in the output wells of these devices. The inclusion of the additional oil barrier reduced the MCF-7 recovery from 70% to 59%, a level similar to other reports involving the extraction of spiked cancer cells into blood (Xia et al. 2006).

While immunocapture methods are routinely utilized to manipulate cell populations without significant lysis, the effect of the oil traverse on cell viability is not commonly tested. In order to investigate cell viability, MCF-7 cells were drawn through the oil barrier, collected from the output well via micropipette, and cultured in a 96-well plate. Cells were observed to adhere to the well plate surface and proliferate over the course of several days (Fig. 5). Staining of dead cells indicated that a similar minority subpopulation of cells had died for both IFAST-sorted cells and unsorted cells (positivecontrol). Over the course of a four-day culture, IFAST-sorted cells increased by 5-fold in number, a value statistically indistinguishable (p=0.66) from proliferation measurements collected from cells that had not

traversed an oil barrier. Together, these data suggest that the cells can be drawn through oil barriers with nominal lysis or cell death and that the cells retain their ability to proliferate. In fact, the collapse of the aggregate into a tight, spherical shape as it enters the oil (as in Fig. 2(b)) suggests that the aggregate interstitial space contains aqueous material from the input well as the spherical shape minimizes the surface energy associated with the aqueous / oil interface. Thus, the cells in the aggregate, particularly those in the interior of the aggregate, are not directly exposed to oil at any point during the separation. However, even after washing with media and passaging with trypsin, some cells remained attached to the PMPs which may affect certain downstream applications (as is the case with other magnetic bead-based technologies). Alternatively, cells could be sorted using negative selection (i.e., pulling unwanted cells through the oil barrier, leave the desired cells isolated in the input well) or using PMPs with a cleavable linkage such as Dynabeads CELLection™ or FlowComp™ (Invitrogen).

In summary, we have applied immiscible phase filtration to cell sorting, resulting in a platform (Fig. 1) with a distinct set of advantages beyond traditional magnetic cell sorting processes. The device is simple, each consisting of three interconnected wells (an input well, an immiscible phase well, and an output well) configured to mimic a 384-well plate footprint (Fig. 1(d, e)). The device operates in a batch processing mode, isolating several thousand cells simultaneously, and can be arrayed, due to the simplicity of the device, to further accelerate throughput. Operation is very straightforward and only requires a handheld magnet to draw PMP-labeled cells through the oil phase and into the output region. In this manner, cells are isolated with a high yield and purity, which is further improved by linking multiple barriers in series. Additionally, no material is washed away or diluted during isolation, allowing the analysis of both negatively and positively selected cells. The negative selection fraction can be directly recovered from the input well following operation of the device; this fraction will not be diluted in wash buffer (as with traditional magnetic bead approaches) nor will it be transferred out of the IFAST device during positive selection, thus limiting loss associated with handling. The positive selection fraction will not be exposed to the multiple washing steps that have been shown to wash away target cells in a significant and variable way. While the magnitude and variability of loss is likely dependent on the antibody/antigen system employed to couple the PMPs to the target cells, we feel that the MCF-7 model system illustrates a weakness of washing-based methods, particularly when quantitative results are desired (i.e., significantly more cells were lost when using vigorous washing compared to gentle washing). Lastly, IFAST-purified cell populations remain intact and viable as they traverse the immiscible phase, enabling analysis by downstream applications.

4 Conclusions

The IFAST platform enables rapid, arrayed isolation of target cells from an aqueous sample. PMP-labeled cells were selectively drawn across an immiscible phase barrier, resulting in an approximately 100-fold reduction in contaminant concentration. Further purity was obtained by traversing two immiscible phase barriers in series, an enhancement that does not significantly increase the complexity or time-to-purification of the system. This improvement in performance occurred because the contaminant particles trapped in the interstitial space of the PMP/cell aggregate could be released in a wash buffer following the first oil barrier traverse. The process was effective for both dense concentrations of cells (>50% of total particles) as well as minority sub-populations (<10% of total particles) and more cells were recovered with less variance when compared to traditional washing-based methods. Furthermore, cells remained intact and viable after traversing the oil barrier, as indicated by live/dead staining and their ability to proliferate.

The capability of the IFAST platform to rapidly, simply, and efficiently separate sub-populations of cells could potentially facilitate the application of a wide variety of downstream analyses, including cellular enumeration, gene expression analysis, and protein quantification, to a difficult-to-process class of biological samples – mixed cell populations. The IFAST platform could potentially be employed to segregate mixed cell populations in co-culture experiments, such as those investigating the effects of stromal interactions on tumor cell behavior. The platform could also serve as a more economical alternative to flow cytometry-based cell separations. Additionally, tissue specimens could be processed with the IFAST technology prior to downstream analysis and/or culture, aiding the capture of purified cell populations for clinical diagnostics.

Supplementary Material

Refer to Web version on PubMed Central for supplementary material.

Acknowledgments

This work was funded by the University of Wisconsin Stem Cell and Regenerative Medicine Center, the Walter H. Coulter Translational Research Partnership, National Institutes of Health Grant #5R33CA137673, and Department of Defense BCRP Concept Award #W81XWH-08-1-0525. J.D. Kueck is a Mary Engsberg Fellow. A portion of this work was funded by DHS Science and Technology Assistance Agreement No. 2007-ST-061-000003 awarded by the U.S. Department of Homeland Security. It has not been formally reviewed by DHS. The views and conclusions contained in this document are those of the authors and should not be interpreted as necessarily representing the official policies, either expressed or implied, of the U.S. Department of Homeland Security. The Department of Homeland Security does not endorse any products or commercial services mentioned in this publication.

References

Abramoff MD, Magelhaes PJ, Ram SJ. Biophotonics Int. 2004; 11:36e42.

Atencia J, Beebe DJ. Nature. 2005; 437:648–655. [PubMed: 16193039]

Berry SM, Alarid ET, Beebe DJ. Lab Chip. 2011; 11:1747–1753. [PubMed: 21423999]

Bhagat AAS, Bow H, Hou HW, Tan SJ, Han J, Lim CT. Med. Biol. Eng. Comput. 2010; 48:999–1014. [PubMed: 20414811]

Bordelon H, Adams NM, Klemm AS, Russ PK, Williams JV, Talbot HK, et al. Appl. Mater. Interfaces. 2011

Chen H, Abolmatty A, Faghri M. Microfluid. Nanofluid. 2010; 10:593–605.

Cho H, Kim H-Y, Kang JY, Kim TS. J. Colloid Interface Sci. 2007; 306:379–385. [PubMed: 17141795]

Fu AY, Spence C, Scherer A, Arnold FH, Quake SR. Nat. Biotechnol. 1999; 17:1109–1111. [PubMed: 10545919]

Hu X, Bessette PH, Qian J, Meinhart CD, Daugherty PS, Hyongsok ST. PNAS. 2005; 102:15757–15761. [PubMed: 16236724]

Huang LR, Cox CE, Austin RH, Sturm JC. Science. 2004; 304:987–990. [PubMed: 15143275]

Kelso, DM.; Sur, K.; Parpia, Z. United States Patent Application. Application #12/395020. 2009.

Lenshof A, Laurell T. Chem. Soc. Rev. 2010; 39:1203–1217. [PubMed: 20179832]

MacDonald MP, Spalding GC, Dholakia K. Nature. 2003; 426:421–424. [PubMed: 14647376]

Miltenyi S, Muller W, Weichel W, Radbruch A. Cytometry. 1990; 11:231–238. [PubMed: 1690625]

Nagrath S, Sequist LV, Maheswaran S, Bell DW, Irimia D, Ulkus L, et al. Nature. 2007; 450:1235–1241. [PubMed: 18097410]

Pamme N. Lab Chip. 2005; 6:24–38. [PubMed: 16372066]

Pamme N, Manz A. Anal. Chem. 2004; 76:7250–7256. [PubMed: 15595866]

Petersson F, Aberg L, Sward-Nilsson A-M, Laurell T. Anal. Chem. 2007; 79:5117–5123. [PubMed: 17569501]

Shikida M, Takayanagi K, Honda H, Ito H, Sato KJ. Micromech. Microeng. 2006; 16:1875–1883.

Sur K, McFall SM, Yeh ET, Jangam SR, Hayden MA, Stroupe SD, Kelso DM. J. Mol. Diagno. 2010; 12:620–628.

Symmans WF, Ayers M, Clark EA, Stec J, Hess KR, Snelge N, et al. Cancer. 2003; 97:2960–2971. [PubMed: 12784330]

Tsutsui H, Ho C-M. Mech. Res. Commun. 2009; 36:92–103. [PubMed: 20046897]

Wildings P, Kricka LJ, Cheng J, Hvichia G, Shoffner MA, Fortina P. Anal. Biochem. 1998; 257:95–100. [PubMed: 9514776]

Xia N, Hunt TP, Mayers BT, Alsberg E, Whitesides GM, Westervelt RM, et al. Biomed. Microdevices. 2006; 8:299–308. [PubMed: 17003962]

Yamada M, Nakashima M, Seki M. Anal. Chem. 2004; 76:5465–5471. [PubMed: 15362908]

Zhao B, Moore JS, Beebe DJ. Science. 2001; 291:1023–1026. [PubMed: 11161212]

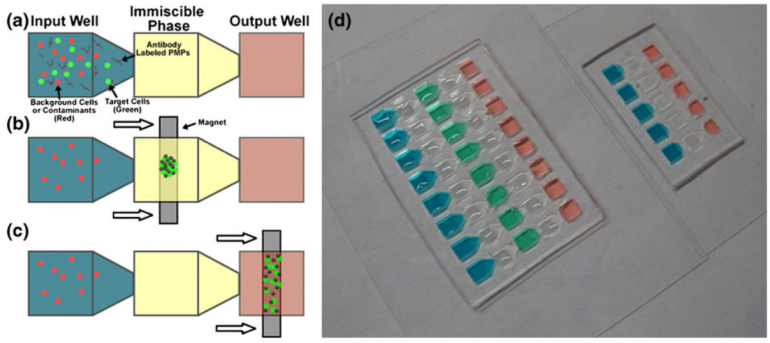

Fig. 1.

Photograph of IFAST devices and schematic of operation. (**a**) MCF-7-eGFP cells that have had time to bind to anti-EpCAM labeled PMPs with red fluorescent particles are added to the input well. The immiscible phase is oil. The output well contains 1% PBS. (**b**) An external magnet is used to draw the MCF-7-eGFP cells bound to anti-EpCAM labeled PMPS through the oil (**c**) Next the MCF-7-eGFP cells are pulled to the output well for further downstream applications (**d**) Photograph of single IFAST (right) and double IFAST (left) loaded with colored reagents and oil (clear)

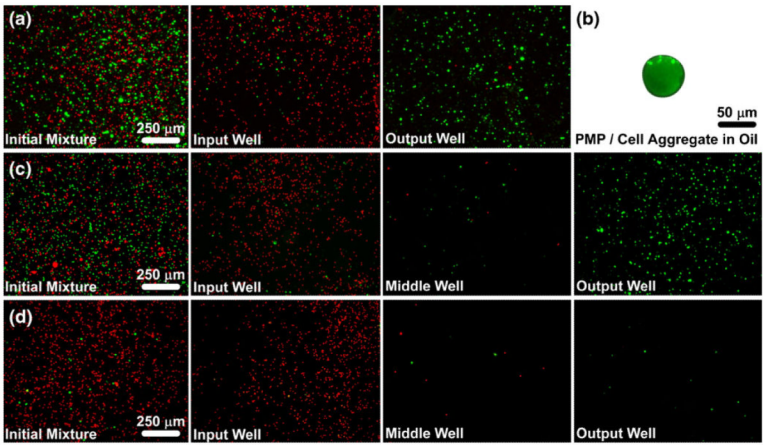

Fig. 2.

Selective isolation of green fluorescent MCF-7 cells from red fluorescent particles. (**a**) A mixture of cells (green), particles (red) and anti-EpCAM-labeled PMPs were added to an IFAST device, which was used to transfer the cells to the output well of the device while leaving most of the particles in the input well. (**b**) The PMPs and cells form a tight aggregate as they cross the oil phase, thus minimizing carryover of extraneous material, such as the particles. (**c**) The same sample from A was purified using an IFAST device with two oil barriers in series with a washing buffer located between them. The double oil barrier increases purity since nearly all of the contaminating particles that cross the first oil barrier do not cross the second oil barrier. (**d**) An additional IFAST with two oil barriers was loaded with a mixture containing approximately 10× fewer cells than in A and B. The double oil barrier is suitable for isolating small cell numbers with minimal contamination. A, C, and D were taken at 4× magnification while B was taken at 20× magnification. Images of input, middle, and output wells were taken after IFAST purification

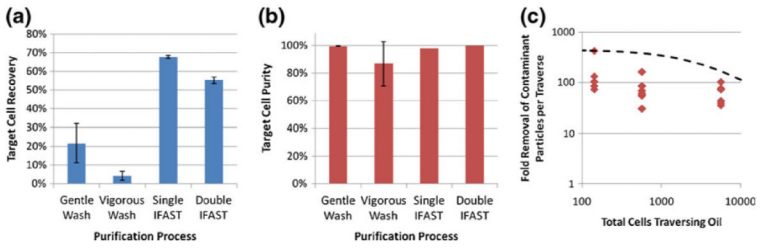

Fig. 3.

Performance of the IFAST platform. (**a**) Total cell recovery as a function of purification process. Cell/particle mixtures were purified using gentle washing, vigorous washing, single oil barrier IFAST, or double oil barrier IFAST, and cells in output well were counted and compared against initial numbers. Recovery is significantly higher when using the IFAST devices compared to the washing techniques ($p<0.05$ when comparing either IFAST device to either washing technique). (**b**) In the same experiment as A, particles in the output well were counted to determine purity using Eq. 1. Purity is consistently high for all methods, but with higher variance when using vigorous washing. The purity when using two oil barriers is significantly higher than with one oil barrier (99.7% vs. 97.9%; $p< 0.005$). (**c**) Oil traverse results in a 30 to 400-fold reduction in particle concentration, which was calculated by measuring the number of particles in the output well and dividing by the total initial number of particles in the sample. These data approach the theoretical purification limit (as defined by Eq. 2) when the PMP / cell aggregates are assumed to be in the close-packed sphere configuration

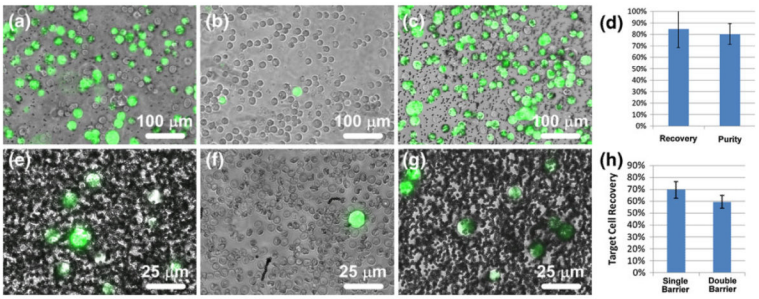

Fig. 4.

Separation of MCF-7 cells (green) from HS-5 cells (uncolored) and whole human blood. An initial mixture (**a**) containing approximately 43% MCF-7 cells and 57% HS-5 cells was sorted via single barrier IFAST and the numbers of each cell type in the input and output wells were counted. The majority (average of 89%) of HS-5 cells were left in the input well (**b**) while most (average of 85%) of the MCF-7 cells were transferred to the output well (**c**). (**d**) The recovery level of the sorted MCF-7 cells and purity of the output well are similar to values observed in the characterization experiments. When MCF-7 cells were sorted from whole blood using a single barrier IFAST device, a significant number of blood cells were transferred to the output well (**e**). When using a double barrier IFAST device, the majority of these cells were released in the middle well ((**f**), a single MCF-7 cell surrounded primarily by red blood cells), resulting in a relatively pure sample in the output well (**g**). When a second oil traverse was added, recovery was reduced from 70% to 59% (**h**). Due to the low concentration of MCF-7 cells, lots of unbound PMPs are seen in Image E and G. (Note the dark dots in (**g**) are unbound PMPs, not contaminant cells.) Images A-C were obtained using a 10× objective while images E-G were obtained with a 40× objective. The input wells of IFAST devices used for the blood sorting experiments were too densely populated with blood cells to image

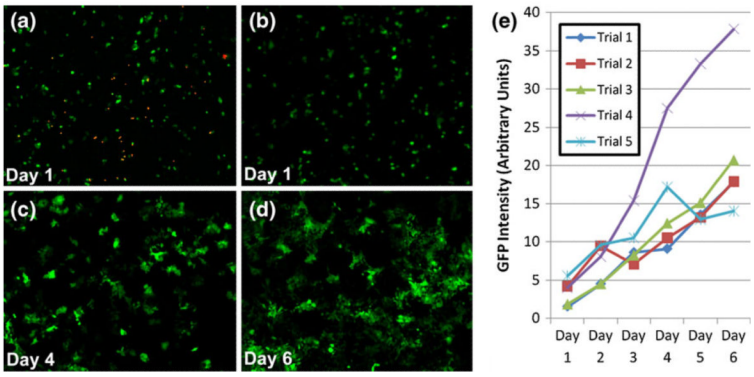

Fig. 5.

Viability of GFP-positive MCF-7 cells following traverse through oil barrier. (**a**) Cells seeded into 96-well plate following oil traverse and stained to highlight dead cells (orange). (**b**-**d**) Proliferation of MCF-7 cells in 96-well plate following traverse through the oil barrier. Images taken at 1, 4, and 6 days after traverse, respectively. (**e**) Quantification of GFP signal for five independent trials where MCF-7 cells were drawn across oil barrier and seeded into wells of a 96-well plate. Note that GFP intensity is proportional to cell number (Fig. S-1)